

Proton MAS NMR Spectra at High Magnetic Fields and High Spinning Frequencies: Spectral Simulations Using Floquet Theory

Siddharth Ray, Elena Vinogradov, Gert-Jan Boender, and Shimon Vega

Department of Chemical Physics, The Weizmann Institute of Science, 76100 Rehovot, Israel

Received January 9, 1998; revised June 9, 1998

Proton magic angle spinning (MAS) spectra of a model spin system, consisting of six protons, were calculated for different values of the external magnetic field and the spinning frequencies. Floquet theory was used to evaluate these spectra. The reduction of the effective homonuclear dipolar interaction for increasing spinning frequency was investigated. The influence of an increase of the external magnetic field and the spinning frequencies on the linewidths of the centerband spectra is discussed. This Floquet description of the rotating proton spin system will assist us in our calculations of the CPMAS spin dynamics of a low abundant spin interacting with a set of coupled protons. © 1998 Academic Press

INTRODUCTION

Using proton spectra in NMR studies of solids has become increasingly popular. In particular because of commercially available high-spinning-frequency rotors and the tendency to exploit high magnetic fields, it has become more attractive to use proton magic angle spinning (MAS) NMR of polycrystalline and amorphous materials. Proton MAS spectra obtained at high spinning rates and high fields exhibit significant line narrowing (1). The combination of multiple-pulse NMR and MAS can result in high-resolution spectra (2) and in recent publications this approach has been extended and improved (3). The frequency-switched Lee–Goldburg (4) has provided an alternative approach for detecting high-resolution spectra and lately it has been implemented in two-dimensional MAS experiments (5). In a recent application of proton NMR, double-quantum sideband spectra have been detected for structural elucidations (6).

Development of novel proton line-narrowing techniques and cross-polarization methods in MAS NMR requires a theoretical framework to describe these experiments. In order to better understand the spin evolution of a set of coupled protons rotating at the magic angle in a high external magnetic field, we suggest the use of the Floquet description of this spin system (7, 8). The magnetic field and spinning frequency dependence of Floquet state energies, in particular, can be followed and interpreted in terms of a reduction of the effective homonuclear interaction in the rotating proton system. This reduction was discussed recently, while describing CPMAS experiments on an $S(1/2)I_N$ spin system using Floquet theory (9). The changes in the Floquet energies for increasing spinning frequency result

in the narrowing of the proton linewidths. Maricq and Waugh (10) in their pioneering paper on MAS NMR discussed the dependence of the linewidths of a homonuclear spin system on the spinning frequency and derived an inverse proportionality. Levitt *et al.* (11) extended the discussion and showed that this dependence can become stronger and can reach an inverse square dependence at high spinning frequencies. Wind has shown that the experimental proton linewidth of a variety of compounds is inversely proportional to the spinning frequency (12). Simulations of MAS spectra of two- and three-spin homonuclear spin systems were extensively studied and the residual broadening of their center and sidebands for varying spinning frequencies was reported (11, 13–15).

Here we consider a six-proton spin system and demonstrate the use of the Floquet approach for calculating its proton MAS spectrum. In the next section we provide the theoretical background for the Floquet description of a set of coupled protons, rotating at the magic angle in a high magnetic field. The matrix elements of the proton Floquet Hamiltonian are derived and the diagonalization procedure of this Hamiltonian is shown. In the third section the methodology for calculating the spectra is presented as well as some results. In the last section these results are discussed and some comments are made about their significance for further research.

THEORETICAL BACKGROUND

The rotating frame Floquet Hamiltonian (7, 9, 16) describing a homonuclear spin system can be represented in a set of dressed spin states $|M_p n\rangle$, where $|M_p\rangle$ is one of the $p = 1, \dots, n_M$ spin states with a z component of the total spin angular momentum equal to M and $n = -\infty, \dots, \infty$ are the Fourier indexes. The number of individual states in each manifold of states $\{|Mn\rangle\}$ for a fixed M value depends on the number of spins in the system and the number of Fourier indexes, $n = -n_f, \dots, n_f$. For a set of N spins, each M manifold contains $n_M = N!/(N - (M + N/2))!(M + N/2)!$ spin states. The number of Fourier indices of the truncated Floquet matrix must be determined empirically. For example, this can be done by following the convergence of the simulated spectrum for increasing $N_f = 2n_f + 1$ values.

In the rotating frame the Hamiltonian has only nonzero

matrix elements inside the $\{|Mn\rangle\}$ manifolds (9). There are three types of elements: (i) the diagonal elements, which are equal to n times the spinning frequency plus a sum of isotropic chemical shift $h_0^i(M_p)$ and j -coupling values j^{ij}

$$\langle M_p n | H_F | M_p n \rangle = n\omega_R + \sum_i h_0^i(M_p) + \sum_{i < j} \alpha^{ij}(M_p) j^{ij}; \quad [1]$$

(ii) the off-diagonal elements that are a sum of chemical shift anisotropy terms $h_k^i(M_p)$ and the secular dipolar interaction terms a_k^{ij} ,

$$\langle M_p n | H_F | M_p n + k \rangle = \sum_{i < j} h_k^i(M_p) + \alpha^{ij}(M_p) a_k^{ij}, \quad [2]$$

with $\alpha^{ij}(M_p) = \pm \frac{1}{4}$ according to $\langle M_p | I_{zi} I_{zj} | M_p \rangle = \pm \frac{1}{4}$, and (iii) the off-diagonal elements that are equal to one of the flip-flop terms a_k^{ij} of the nonsecular part of the dipolar interaction and the j -coupling,

$$\langle M_p n | H_F | M_q n + k \rangle = \sum_{i < j} \alpha^{ij}(M_{pq}) \{ a_k^{ij} - 2j^{ij} \delta_{k0} \}, \quad [3]$$

with $p \neq q$ and $\alpha^{ij}(M_{pq}) = 0$, $-\frac{1}{4}$ according to $\frac{1}{4} \langle M_p | I_i^+ I_j^- + I_i^- I_j^+ | M_q \rangle = 0$, $\frac{1}{4}$. The chemical shift and dipolar interaction terms are nonzero for $k = -2, -1, 0, 1, 2$. The actual values of the h and a elements can easily be evaluated for a spin system with well-defined chemical shift parameters and atomic positions. The dipolar terms are inversely proportional to the third power of the internuclear distances and are functions of the relative orientations of these vectors with respect to the rotor frame (16),

$$\begin{aligned} h_0^i(M_p) &= m_i^p \delta_i \\ h_k^i(M_p) &= \frac{1}{2} m_i^p \sigma_i g_{|k|}^i \exp\{i\psi_k^i\}, \\ a_k^{ij} &= \frac{\gamma^2 \mu_0 \hbar}{4r_{ij}^3} G_{|k|}^{ij} \exp\{ik\phi_{ij}\}, \end{aligned} \quad [4]$$

where m_i^p is $\pm 1/2$, according to the value of the z component of the angular momentum of spin i in $|M_p\rangle$, and the g and G coefficients and the angles ψ_k^i are real geometric functions of the initial Euler angles (α, β, γ) of the chemical shift tensors and the polar angles (θ, φ) of the dipolar vectors \mathbf{r} in the rotor frame, respectively. The δ and σ parameters are the isotropic and anisotropic chemical shift values of the spins with a magnetogyric ratio γ . The chemical shift parameters and the secular terms of the dipolar interaction are all diagonal in M_p , whereas the nonsecular flip-flop terms are off-diagonal. These last terms are the source of the homonuclear line broadenings in the proton MAS spectra and complicate their evaluation. As we are interested only in proton MAS spectra, no radiofrequency terms are considered in the Hamiltonian.

This Floquet Hamiltonian is used for evaluating MAS spectra of N coupled spins. Although in a real sample the number of coupled spins is very large, for practical reasons we must restrict ourselves to the proton spectrum of a single small molecule. A calculation considering only one molecule would correspond to a real system of ordered molecules in which the intermolecular couplings are ignored, or a single molecule in a nonprotonated environment.

SIMULATIONS OF PROTON MAS SPECTRA

To evaluate the proton spectrum of an N -proton system the Floquet Hamiltonian matrix elements must be calculated and the truncated representations of its $(n_M \cdot N_f) \times (n_M \cdot N_f)$ diagonal blocks in the $\{|Mn\rangle\}$ manifolds must be constructed for all M values. Here the value of N_f is determined by monitoring the convergence of the principal eigenvalues. Each M block matrix must be diagonalized to obtain a set of eigenvalues and eigenvectors of the form (9)

$$\begin{aligned} \lambda_n^p(M) &= \lambda_0^p(M) + n\omega_R \\ |\lambda_n^p(M)\rangle &= \sum_{m=-N_f}^{N_f} \sum_{q=1}^{n_M} |M_q m\rangle \langle M_q m | D | \lambda_n^p(M) \rangle, \end{aligned} \quad [5]$$

with $\lambda_0^p(M)$ and $|\lambda_0^p(M)\rangle$ being the principal eigenvalues and eigenvectors (7), respectively, and D the diagonalization matrix of the Floquet Hamiltonian. The proton spectrum can then be evaluated by determining the frequencies and amplitudes of the allowed transitions of the spin system. To do so the normalized matrix elements of the signal operator between the $|\lambda_n^p(M)\rangle$ and $|\lambda_0^q(M+1)\rangle$ states must be calculated. The nonzero elements of this operator \mathbf{M}_0 , in the original Floquet state representation, are

$$\langle M_p n | \mathbf{M}_0 | (M+1)_q n \rangle = \langle M_p | \sum_{i=1}^N I_i^- | (M+1)_q \rangle \quad [6]$$

and the free induction decay signal becomes (7, 16)

$$S(t) = \sum_M \sum_{p < q} \sum_n S_n^{pq} \exp\{i(\lambda_n^p - \lambda_0^q)t\} \quad [7]$$

and

$$\begin{aligned} S_n^{pq} &= \left\{ \sum_m \langle \lambda_m^p(M) | D^{-1} \mathbf{M}_0 D | \lambda_0^q(M+1) \rangle^* \right. \\ &\quad \left. \times \langle \lambda_n^p(M) | D^{-1} \mathbf{M}_0 D | \lambda_0^q(M+1) \rangle \right\}. \end{aligned} \quad [8]$$

A sequential diagonalization of the Floquet block matrices, for all M values, and a calculation of the frequencies and ampli-

TABLE 1

The Proton Coordinates in Arbitrary Molecular Reference Frame and Chemical Shift Values for the Two Model Molecules $\text{CD}_2\text{H}^a\text{—CH}_2^b\text{—CH}^c\text{=CH}^d\text{—CH}^e\text{O}$ and $\text{CH}_2^x\text{—CH}_2^y\text{—CH}_2^z$

	x (Å)	y (Å)	z (Å)	δ (ppm)
H^a	2.81	-0.35	-8.76	1.2
H^{1b}	5.20	0.31	-8.96	2.0
H^{2b}	4.75	0.04	-7.26	2.0
H^c	4.29	2.92	-7.86	6.0
H^d	7.01	1.56	-7.36	6.5
H^e	5.97	4.63	-7.15	9.5
H^{1x}	3.0	1.7	-0.9	0.0
H^{2x}	3.0	1.7	0.9	0.0
H^{1y}	1.9	3.9	-0.9	2.0
H^{2y}	1.9	3.9	0.9	2.0
H^{1z}	4.4	3.7	-0.9	6.0
H^{2z}	4.4	3.7	0.9	6.0

tudes, following Eqs. [7] and [8], for a set of randomly oriented molecules result in a MAS proton powder spectrum.

To demonstrate the field and spinning frequency dependence of the proton MAS spectra a set of simulations was performed. For these calculations a FORTRAN program based on the procedure discussed above was written. Its input parameters are proton coordinates, isotropic chemical shifts, and a 121-kHz dipolar-coupling strength for a pair of protons with separation of 1 Å. We simulated spectra for a system of six coupled protons in a system with a structure similar to a *d*₂-*trans*-2-pentenal molecule



with isotropic chemical shift values

$$\delta_a = 1.2 \text{ ppm}, \delta_b = 2 \text{ ppm}, \delta_c = 6 \text{ ppm},$$

$$\delta_d = 6.5 \text{ ppm}, \delta_e = 9.5 \text{ ppm}.$$

In Table 1 the proton coordinates of the molecule in an arbitrary reference frame are summarized. This model system contains protons with chemical shifts that are spread over a range of more than 8 ppm. It consists of one CH₂ group, one CHO group with a chemical shift that is 3 ppm removed from the other protons, and three CH groups with chemical shift values ranging from 1.2 to 6.5 ppm. To simplify the calculations, no chemical shift anisotropy parameters and heteronuclear interactions were taken into account.

Proton spectra of our model system were simulated and some results are shown in Figs. 1 and 2. In the calculations the M block Floquet matrices were constructed with $N_f = 21$. For $N = 6$ the number of states n_M are 1, 6, 15, 20, 15, 6, and 1 for $M = 3, 2, 1, 0, -1, -2,$ and -3 , respectively. Although all spectra exhibited significant sideband intensities, only the central part of the spectra are shown. The spectra were ob-

tained by a summation of the frequency spectra of 300 single molecules with varying Euler angles (α, β, γ), between an arbitrary molecular frame and the rotor frame, determined by Conroy's integration method (17). In our powder calculation no initial analytic integration was performed over the time-dependent Euler α angle (18). All spectra were convoluted by a Lorentzian broadening function with a width of 60 Hz. The frequency resolution of the spectra was 20 Hz. The nonzero j -coupling constants that are smaller than 10 Hz did not influence these spectra significantly. The CPU time for a full powder calculation of six spin systems was 4 h on an ALPHA DEC workstation.

Figure 1 shows the combined effect of an increase of the magnetic field and the spinning frequency. At high field and spinning frequencies the line at 9.5 ppm is significantly resolved from the other lines. However, the $\text{CH}^c\text{=CH}^d$ and $\text{CH}^a\text{—CH}_2^b$ lines, with chemical shift separations in the range of 1.2 to 2.0 ppm, are not resolved. In particular the H₂ protons exhibit a significant residual broadening even at 800 MHz. Figure 2 shows the changes in the proton spectrum for an increasing external magnetic field at a fixed spinning frequency of 20 kHz.

The spectra are composed of many allowed transitions

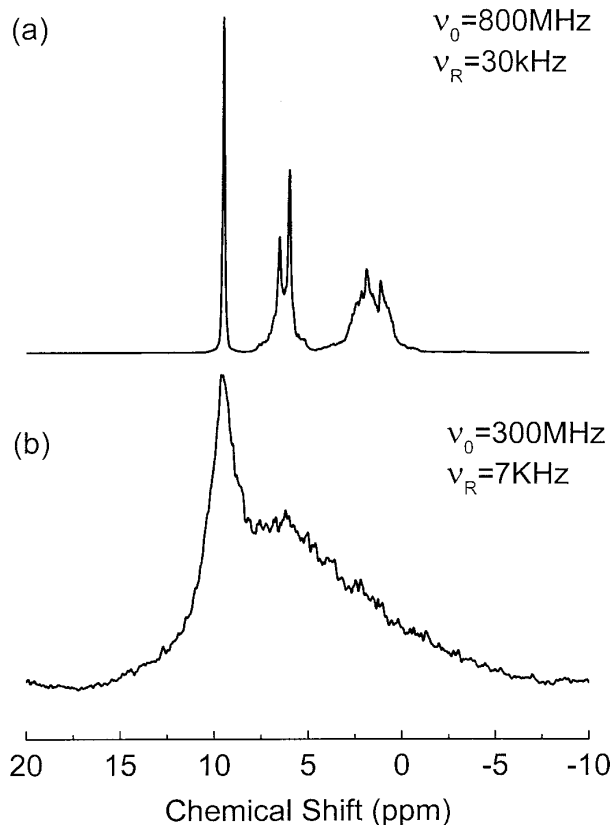


FIG. 1. The simulated proton MAS powder spectrum of the $\text{CD}_2\text{H—CH}_2\text{—CH=CH—COH}$ model molecule (see main text) (a) rotating at a spinning frequency of 30 kHz in an 800-MHz external magnetic field and (b) at a spinning frequency of 7 kHz at a field of 300 MHz. In both spectra only the centerband region is shown.

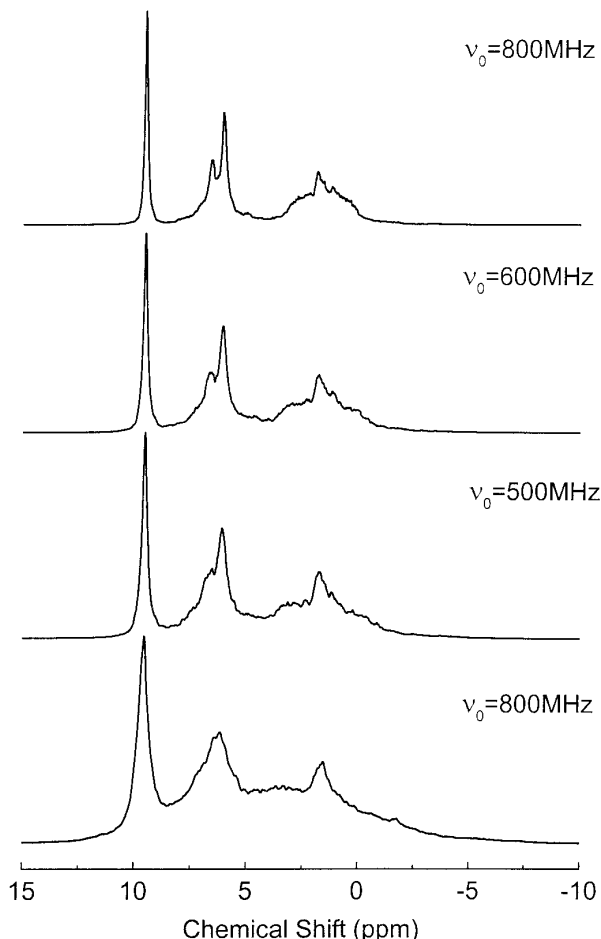


FIG. 2. The calculated field dependence of the proton MAS powder spectrum of the $\text{CD}_2\text{H}-\text{CH}_2-\text{CH}=\text{CH}-\text{COH}$ model molecule rotating at a frequency of 20 kHz.

between Floquet states, and their energies and eigenfunctions are complicated functions of the experimental parameters. Before discussing the spinning frequency dependence of the linewidths in the spectrum, we summarize some of the features of the centerband spectra of one proton and two equivalent protons coupled to an additional proton. In the Appendix the dependence of the proton MAS spectra of H^1-H^2 and H_2^1-H^2 on the value of the spinning frequency and the external magnetic field is evaluated. In this derivation we used Floquet theory together with standard perturbation theory (8). These calculations show that the linewidth of the H^1 centerband is proportional to $1/(\delta_{12}\omega_R^2)$, where δ_{12} is the chemical shift difference in frequency units, as was already shown by Levitt *et al.* (11). The H_2^1 centerband spectrum of a single H_2^1-H^2 spin system is composed of at least eight transitions between the eight principal eigenstates. Their energy dependence on ω_R and δ_{12} differs from state to state. The two eigenvalues with $M = \pm 3/2$ are constant; four of the eigenvalues are about proportional to $1/\omega_R$ and two follow $1/(\delta_{12}\omega_R^2)$. The transitions between the states, and thus the powder spectral widths, do not follow

simple power dependences on the spinning frequency and the chemical shift difference. However, we can conclude that part of the lineshape does not narrow (in frequency units) for increasing magnetic field, while the whole lineshape narrows for increasing spinning frequency.

THE SPINNING FREQUENCY DEPENDENCE OF THE LINEWIDTHS

To investigate the reduction of the homonuclear interaction during MAS experiments we evaluated the proton linewidths as a function of the spinning frequency $\nu_R = \omega_R/2\pi$. In Fig. 3 the full widths at half-height $\Delta\nu(\nu_R)$ of the proton centerbands are drawn as a function of ν_R for a field of 300 MHz. The exact positions of the spectral lines in Fig. 3 show small shifts that are functions of the strength of the dipolar interactions and the chemical shift differences of the interacting protons (11, 13–15). The points in this figure are the linewidths calculated for four cases. (a) First the width of the CH^cO line in our model molecule is shown. This line is fully resolved in the proton spectra and can easily be detected. (b) Then the width of the single proton line, which is obtained when all the chemical shift values of our molecule are equal, is drawn. This is followed by proton linewidth calculations for the CH_2 group. For these two equivalent spins two calculations were performed. (c) First the width of the double-quantum spectrum of the CH_2^b protons in our molecule was monitored. The double-quantum spectrum

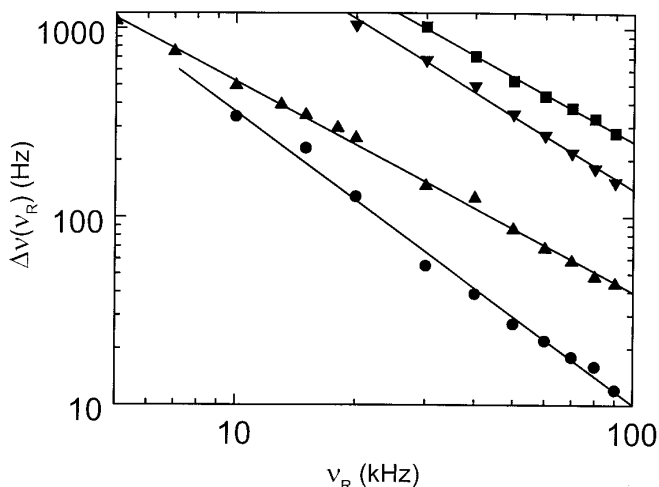


FIG. 3. The spinning frequency dependence of the full linewidths at half-height $\Delta\nu(\nu_R)$ of different protons in the MAS powder spectra of a six-proton spin systems: (a) The circles correspond to the proton line of the CH^cO proton in our model molecule (see main text), (b) the triangles correspond to the proton line of our model molecule with all isotropic chemical shift values equal, (c) the inverted triangles are the calculated results of the linewidths of the double-quantum line of the CH_2^b protons in our model molecule, and (d) the squares belong to the proton line of CH_2^a at 6.0 ppm in a molecule of the form $\text{CH}_2^a-\text{CH}_2^b-\text{CH}_2^c$ with chemical shifts $\delta_a = 0.0$ ppm, $\delta_b = 2.0$ ppm, and $\delta_c = 6.0$ ppm. The straight lines through the points have slopes equal to -1.5 , -1.1 , -1.3 , and -1.1 , respectively.

was calculated by assuming an initial double-quantum spin density operator with matrix elements

$$\langle M_p n | R(t) | (M \pm 2)_{q n} \rangle = \langle M_p | (I_b^+)^2 + (I_b^-)^2 | (M \pm 2)_q \rangle \quad [9]$$

and a signal operator

$$\langle M_p n | \mathbf{M}_0^2 | (M + 2)_{q n} \rangle = \langle M_p | (I_b^-)^2 | (M + 2)_q \rangle. \quad [10]$$

This spectrum exhibits a centerband and sidebands with significant intensities. The widths of the center and sidebands are governed by the interactions between the H_2^b protons and the remaining protons. The interaction between the two protons alone does not cause any broadening of the MAS spectrum. Thus the width represents the presence of the effective interaction between the CH_2^b protons and the rest of the molecule. (d) Finally we evaluated the CH_2 proton linewidth of the single-quantum line of the CH_2^y proton pair in a molecule of the form $CH_2^x-CH_2^y-CH_2^z$, with chemical shifts $\delta_x = 0$ ppm, $\delta_y = 2.0$ ppm, and $\delta_z = 6.0$ ppm. The proton coordinates are listed in Table 1. The straight lines through the calculated points in Fig. 3 follow

$$\log\{\Delta\omega(\omega_R)\} = \log\{A\omega_R^{-x}\} \quad [11]$$

and have slopes $1.1 < x < 1.5$. A study of the dependence of the A coefficient in Eq. [11] on experimental parameters is underway.

The x values for the protons in the molecule with equal isotropic chemical shifts (b) and the CH_2^y in $CH_2^x-CH_2^y-CH_2^z$ (d) are close to the experimental values $x = 1.0 \pm 0.1$ obtained by Wind (12). The terminal proton of CH^eO in the model molecule (a) shows an increased slope of $x = 1.5$.

Maricq and Waugh (10), using Average Hamiltonian Theory, explained the inverse proportionality of the widths as a function of the spinning frequency. Levitt *et al.* (11) discussed the $\{1/\omega_R\}^2$ dependence. Our results show x values smaller than 2, even for the CH^eO line, which indicates the complexity of the homonuclear coupling in multispin systems. To investigate the origin of the changes in the linewidths somewhat more, we followed the principal eigenvalues of the Floquet Hamiltonian of our proton system, at some fixed orientation in the rotor and at an external field of 300 MHz, as a function of the spinning frequency. Figures 4 and 5 show the results of this calculation. These values were obtained by numerical diagonalization of the M block matrices with $N_f = 21$. Figure 4 plots the energies for $M = -2, -1, 0$. The approach of all of these energies to their asymptotic values at infinite spinning frequency $\lambda_0^p(M_p, \infty) = h_0(M_p)$ was calculated, assuming that all the j couplings were zero. Most of the energy values follow Eq. [11]. An example is shown for $M = -2$ in Fig. 4d. In order to explain this result in terms of the Floquet description of the spin system it would be necessary to derive some analytic expressions for the eigenvalues based on perturbation theory. This is not trivial because of the large size of the

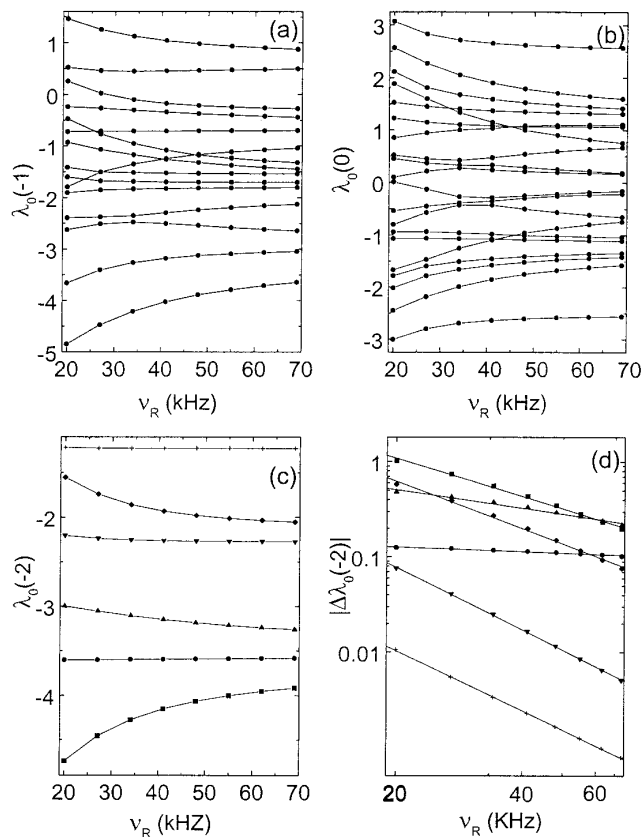


FIG. 4. The spinning frequency dependence of the $n = 0$ MAS Floquet energies of a single crystallite of the six-proton model molecule, at an arbitrary orientation in the rotor frame. The energies are divided according to their M values: (a) $M = -1$, (b) $M = 0$, and (c) and (d) $M = -2$. The dots are the calculated values and the solid lines connect them to guide the eye. A magnetic field of 300 MHz was used for these calculations. The energies are drawn as a function of the spinning frequency $\nu_R = \omega_R/2\pi$. To show that almost all energies follow approximately some $\{1/\omega_R\}^x$ dependence, the results of (c) are repeated in (d), where the absolute value of the difference $|\Delta\lambda_0(-2)|$ between the eigenvalue $\lambda_0(-2, \nu_R)$ and its chemical shift values $\lambda_0(-2, \infty)$ is plotted on a logarithmic scale.

matrices. For the three-proton case such a derivation is shown in the Appendix.

The convergence of the Floquet energies shows the effective reduction of the homonuclear dipolar interaction between the protons at high spinning frequencies. To demonstrate this reduction an additional energy calculation was performed assuming equal chemical shift values for all protons in our model compound, and Fig. 5 shows the Floquet energies between the values ± 70 kHz. Clearly, for spinning frequencies larger than 10 kHz, the states with different n values are separated from each other and the energy spread for each n approaches zero for increasing spinning frequency. This reduction in the spread of the Floquet energies influences the efficiencies of the population redistributions during the CPMAS mixing time (9). During these experiments Floquet states are energy matched to allow these population redistributions. This reduction also changes the adiabatic character of the variable amplitude

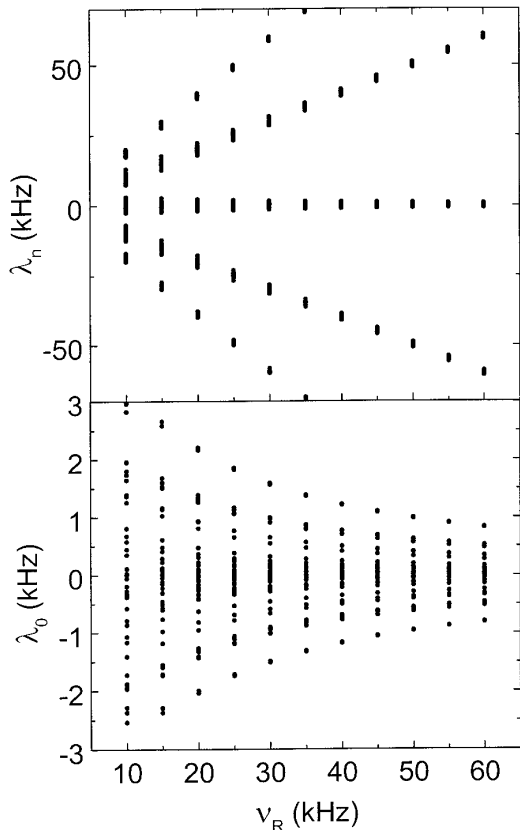


FIG. 5. All Floquet energies between 60 and -60 kHz (top) 4 and -4 kHz (bottom) of a single crystallite of our model molecule, containing six protons all with a chemical shift value equal to zero. The observed spread of the Floquet energies is solely due to the homonuclear interaction. The decrease of these energy spreads represents the effective reduction of the interaction for increasing spinning frequency.

CPMAS experiments (19, 20) and should influence the CP signal enhancement.

DISCUSSION AND COMMENTS

We have studied the field and spinning frequency dependence of the linewidths of the MAS proton spectrum of a six-spin system, using Floquet formalism. We have found that the changes in the Floquet energies and the linewidths of these spectra are proportional to a power of $-x = -1.1 \div -1.5$ of the spinning frequency. In addition we have discussed the reduction of the dipolar line broadening because of chemical shift differences. Our calculations present only a simple model for the MAS proton spectra of a real solid. In real systems many more spins are involved in the spin dynamics governing the free induction decay of the proton coherences. However, the major contribution to the signal decay comes from the short-range proton-proton interactions, in particular, since the interference of coherence modulations is monitored, which causes a decay of the observed signals before a quasi-steady state is reached in the spin system. During modeling spin diffusion processes, long-range interactions, and

indirectly coupled spins are important, because they govern the population rearrangements monitored over long atomic distances (21). The calculated ω_R^{-x} dependence of the linewidths suggests that even at high field and spinning frequencies it is necessary to apply line-narrowing techniques (2, 3) when high-resolution proton spectra are required. Because a part of the principal energies of the proton system is independent of chemical shift differences, increasing the external magnetic field does not reduce the widths (in frequency units) of all the lines in the spectrum, in particular those of equivalent protons. Thus, techniques that take advantage of the line narrowing, that is a result of the high field and spinning frequency, should be developed.

In a successive publication we will discuss the spin dynamics of CPMAS experiments (9, 22) involving a system consisting of a ^{13}C and six protons rotating at a high frequency. These experiments require Floquet energy matching between manifolds of states, such as $\{|M\alpha n\rangle\}$ and $\{|M + 1\beta n + k\rangle\}$, where α and β are the spin states of the carbon atom. The energy spread of these manifolds is an important factor in determining the sensitivity of the CPMAS signal enhancements to mismatched Hartmann-Hahn conditions (22) and of the adiabatic enhancements in ramped variable amplitude CPMAS experiments (19). The dependence of the Floquet energies on the spinning frequency indicates that the effective homonuclear dipolar interaction decreases, but remains significantly far from zero. These reduced interactions play an important role during spin diffusion and CPMAS experiments on samples rotating at high spinning frequencies.

APPENDIX

Here we discuss the spinning frequency dependence of the MAS spectra of two simple spin systems, $\text{H}^1\text{-H}^2$ and $\text{H}_2^1\text{-H}_2^2$, using Floquet theory. In order to simplify the discussion we shall discard the scalar couplings between the protons. The Floquet matrix H_F of the two-proton system has three nonzero diagonal blocks of dimensions N_f , $2N_f$, and N_f with $M = 1, 0$, and -1 for the spin states $\alpha\alpha$, $(\alpha\beta, \beta\alpha)$, and $\beta\beta$, respectively. If the chemical shift values of the protons are δ_1 and δ_2 and all homonuclear dipolar elements are inserted in the Hamiltonian, the matrices represented in the $\{|(M = 1)n\rangle\}$ and $\{|(M = -1)n\rangle\}$ manifolds can be diagonalized straightforwardly, resulting in the principal eigenvalues (7)

$$\lambda_0^{\alpha\alpha} = -\lambda_0^{\beta\beta} = 1/2(\delta_1 + \delta_2). \quad [\text{A1}]$$

The principal eigenvalues of the $\{|(M = 0)n\rangle\}$ block must be calculated by diagonalization. When $\delta = \delta_1 = \delta_2$ the diagonalization of this block is again simple and the eigenvalues become equal to $\lambda_0^{\alpha\beta\pm\beta\alpha} = 0$, independent of the dipolar interaction (15, 16). As a result the central transition frequencies of the MAS spectra of all spin pairs in a powder are equal to $\lambda_0^{\alpha\alpha} - \lambda_0^{\alpha\beta+\beta\alpha} = \lambda_0^{\alpha\beta+\beta\alpha} - \lambda_0^{\beta\beta} = \delta$, and the dipolar powder spectrum consists of sharp center and sidebands as expected (10).

When the chemical shifts differ the diagonalization of the $\{|M=0\rangle n\rangle\}$ block is not trivial and the principal eigenvalues must be obtained by numerical calculation. However, for dipolar matrix elements smaller than the spinning frequency and the chemical shift difference ($\delta_1 - \delta_2$), perturbation theory can be used to estimate the magnitude of the principal eigenvalues. Before doing so we first diagonalize the single $\{|\alpha\beta n\rangle\}$ and $\{|\beta\alpha n\rangle\}$ blocks and obtain the diagonal elements

$$\lambda_0^{\alpha\beta} = -\lambda_0^{\beta\alpha} = 1/2(\delta_1 - \delta_2). \quad [\text{A2}]$$

After these diagonalizations the nonzero off-diagonal elements of H_F become

$$\begin{aligned} \langle \lambda_n^{\alpha\beta} | H_F | \lambda_{n+k}^{\beta\alpha} \rangle &= \sum_{l,m} \langle \lambda_n^{\alpha\beta} | D^{-1} | \alpha\beta m \rangle \langle \alpha\beta m | H_F | \beta\alpha l \rangle \\ &\times \langle \beta\alpha l | D | \lambda_{n+k}^{\beta\alpha} \rangle, \end{aligned} \quad [\text{A3}]$$

where D is the diagonalization matrix of the z blocks $\{|\alpha\beta n\rangle\}$ and $\{|\beta\alpha n\rangle\}$. For large values of ω_R the approximate values of the elements of D are, to first order in $1/\omega_R$, equal to (7)

$$\begin{aligned} \langle \alpha\beta n | D | \lambda_n^{\alpha\beta} \rangle &\cong 1 \\ \langle \alpha\beta n | D | \lambda_{n+m}^{\alpha\beta} \rangle &\cong \frac{\langle \alpha\beta n | H_F | \alpha\beta n + m \rangle}{m\omega_R}. \end{aligned} \quad [\text{A4}]$$

Insertion of these expressions in Eq. [A3] indicates that the most important elements of the transformed Floquet matrix are proportional to $1/\omega_R$

$$\begin{aligned} \langle \lambda_n^{\alpha\beta} | H_F | \lambda_n^{\beta\alpha} \rangle &= \langle \lambda_n^{\beta\alpha} | H_F | \lambda_n^{\alpha\beta} \rangle \\ &\cong \sum_k 2 \frac{|\langle \alpha\beta n | H_F | \alpha\beta n + k \rangle|^2}{k\omega_R}. \end{aligned} \quad [\text{A5}]$$

The principal eigenvalues of the Floquet matrix can then be estimated by using second order perturbation theory

$$\lambda_0^{\alpha\beta} = -\lambda_0^{\beta\alpha} \cong 1/2(\delta_1 - \delta_2) + \frac{|\langle \lambda_0^{\alpha\beta} | H_F | \lambda_0^{\beta\alpha} \rangle|^2}{(\delta_1 - \delta_2)}, \quad [\text{A6}]$$

and with Eq. [A5] the frequency shifts $\Delta\lambda_i$, defined by $\{(\lambda_0^{\alpha\alpha} - \lambda_0^{\alpha\beta}) - \delta_2\}$, $\{(\lambda_0^{\alpha\alpha} - \lambda_0^{\beta\alpha}) - \delta_1\}$, $\{(\lambda_0^{\beta\beta} - \lambda_0^{\alpha\beta}) - \delta_1\}$, and $\{(\lambda_0^{\beta\beta} - \lambda_0^{\beta\alpha}) - \delta_2\}$, $i = 1, \dots, 4$, respectively, of the centerband lines of a spin pair become proportional to

$$\Delta\lambda_1 \propto 1/(\delta_1 - \delta_2)\omega_R^2. \quad [\text{A7}]$$

Thus, as expected, the bandwidths of the MAS spectrum of a powder is inversely proportional to the chemical shift difference and the square of the spinning frequency ($1/I$).

Figure 6 shows the spinning frequency dependence of the

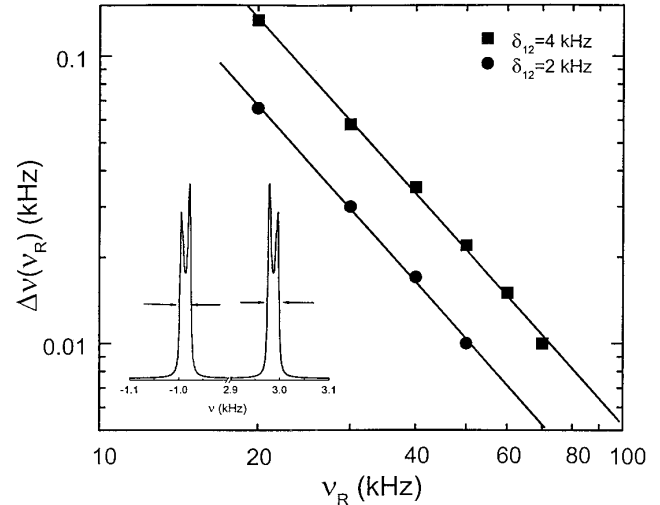


FIG. 6. The calculated dependences of the full widths at half-height of the proton powder lineshapes at the centerband of the MAS spectra of a two-proton system H^1-H^1 , with $r_{12} = 1.5 \text{ \AA}$ and δ_{12} equal to 2 kHz (circles) and 4 kHz (squares). These widths are proportional to $\{1/\delta_{12}\omega_R^2\}$. The slopes of the lines through the calculated points are equal to -2 and the ratio between the widths at 2 and 4 kHz equals 2 for all spinning frequencies.

full width at half-height of the lineshapes at δ_1 and δ_2 of a powder sample of a proton pair with $r_{12} = 1.5 \text{ \AA}$ and a chemical shift difference of 5 ppm, at two external magnetic fields of 400 and 800 MHz, with $\{\delta_1 - \delta_2\}$ equal to 2 and 4 kHz, respectively. The ratio between the widths at these two fields is 2, which is equal to the ratio between the frequency differences, according to Eq. [A7].

To investigate the bandwidths of the lineshapes in the MAS centerband of the three-proton system H_2-H^2 we examine again its Floquet Hamiltonian. The matrix representation of this Hamiltonian consists of four diagonal blocks with $M = 3/2, 1/2, -1/2$, and $-3/2$ of dimensions $N_F, 3N_F, 3N_F$, and N_F , respectively. The centerband lines in the spectra can be divided into five main groups of transitions between the eight principal Floquet energies of these block matrices

$$\begin{aligned} &\lambda_0^1(3/2); \{\lambda_0^1(1/2), \lambda_0^2(1/2), \lambda_0^3(1/2)\}; \\ &\{\lambda_0^1(-1/2), \lambda_0^2(-1/2), \lambda_0^3(-1/2)\}; \lambda_0^1(-3/2) \end{aligned}$$

with chemical shift values

$$\begin{aligned} &\{\delta_1 + 1/2\delta_2\}; \{1/2\delta_2; 1/2\delta_2; (\delta_1 - 1/2\delta_2)\}; \\ &\{-1/2\delta_2; -1/2\delta_2; (-\delta_1 + 1/2\delta_2)\}; \{-\delta_1 - 1/2\delta_2\}, \end{aligned}$$

respectively. The two sets of transitions close to δ_1 are

$$\begin{aligned} (1) &\{\lambda_0^1(3/2) - \lambda_0^1(1/2)\} \quad \text{and} \quad \{\lambda_0^1(3/2) - \lambda_0^2(1/2)\} \\ &\{\lambda_0^1(1/2) - \lambda_0^3(-1/2)\} \quad \text{and} \quad \{\lambda_0^2(1/2) - \lambda_0^3(-1/2)\} \\ (2) &\{\lambda_0^3(1/2) - \lambda_0^1(-1/2)\} \quad \text{and} \quad \{\lambda_0^3(1/2) - \lambda_0^2(-1/2)\} \\ &\{\lambda_0^1(-1/2) - \lambda_0^1(-3/2)\} \quad \text{and} \quad \{\lambda_0^2(-1/2) - \lambda_0^1(-3/2)\} \end{aligned}$$

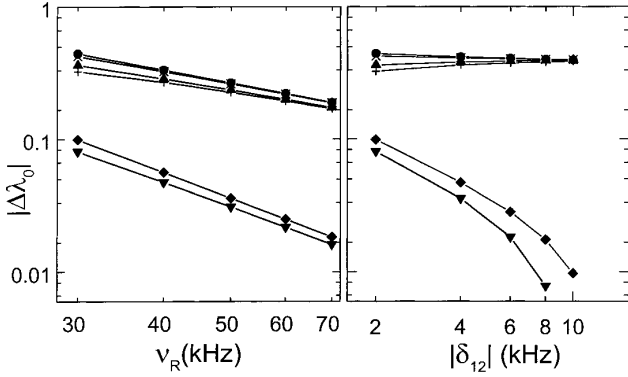


FIG. 7. The shifts of the principal Floquet eigenvalues of a rotating single three-proton system $\text{H}_2^1\text{-H}^2$, placed at some arbitrary orientation in the rotor, as a function of the spinning frequency $\nu_R = \omega_R/2\pi$ and chemical shift difference δ_{12} in units of kHz. Only six of the eight eigenvalues are shown. The two missing values are constant and belong to the $\lambda_0^1(\pm 3/2)$ states. The six values correspond to (●) $\lambda_0^1(-1/2)$, (▲) $\lambda_0^2(-1/2)$, (▼) $\lambda_0^3(-1/2)$, (■) $\lambda_0^1(1/2)$, (×) $\lambda_0^2(1/2)$, and (◆) $\lambda_0^3(1/2)$. The shifts are equal to the differences between the eigenvalues and their chemical shift values $\Delta\lambda_0^i(M) = \lambda_0^i(M, \nu_R) - \lambda_0^i(M, \infty)$. The $\Delta\lambda_0^i(\pm 1/2)$ shifts are proportional to $1/\omega_R^2$ and decay faster than $1/\delta_{12}$ and the $\Delta\lambda_0^i(\pm 3/2)$ shifts are rather independent of δ_{12} and are proportional to $(1/\omega_R)^{0.8-1.0}$.

and the three sets of transitions close to δ_2 are

- (3) $\{\lambda_0^1(3/2) - \lambda_0^3(1/2)\}$
- (4) $\{\lambda_0^1(1/2) - \lambda_0^1(-1/2)\}$ and $\{\lambda_0^1(1/2) - \lambda_0^2(-1/2)\}$
 $\{\lambda_0^2(1/2) - \lambda_0^1(-1/2)\}$ and $\{\lambda_0^2(1/2) - \lambda_0^2(-1/2)\}$
- (5) $\{\lambda_0^3(-1/2) - \lambda_0^1(-3/2)\}$.

In addition to these 14 transitions some low-intensity transitions appear in the spectrum, which are due to mixing between nondegenerate product spin states.

For effectively weak dipolar interactions between the spins, i.e., at high spinning frequencies, the principal eigenstates correspond to the spin states

$$\begin{array}{ll}
 |\lambda_0^1(3/2)\rangle \rightarrow |\alpha\alpha\alpha\rangle & |\lambda_0^1(-1/2)\rangle \rightarrow |\alpha\beta\beta 0 \\
 |\lambda_0^1(1/2)\rangle \rightarrow |\alpha\beta\alpha 0 & |\lambda_0^1(-1/2)\rangle \rightarrow |\beta\alpha\beta 0 \\
 |\lambda_0^2(1/2)\rangle \rightarrow |\beta\alpha\alpha 0 & |\lambda_0^2(-1/2)\rangle \rightarrow |\beta\beta\alpha 0 \\
 |\lambda_0^3(1/2)\rangle \rightarrow |\alpha\alpha\beta 0 & |\lambda_0^3(-3/2)\rangle \rightarrow |\beta\beta\beta 0
 \end{array}$$

(the order of the spin states is chosen according to $\text{H}^1\text{-H}^1\text{-H}^2$). The spinning frequency dependence of the eigenvalues of these states can be estimated by using perturbation theory. The matrix elements of the Floquet block matrices can be evaluated straightforwardly using Eq. [3], and the $M = 3/2$ and $M = -3/2$ blocks can be diagonalized analytically resulting in the principal eigenvalues

$$\begin{aligned}
 \lambda_0^1(3/2) &= 1/2(2\delta_1 + \delta_2) \\
 \lambda_0^1(-3/2) &= -1/2(2\delta_1 + \delta_2).
 \end{aligned}
 \quad [A9]$$

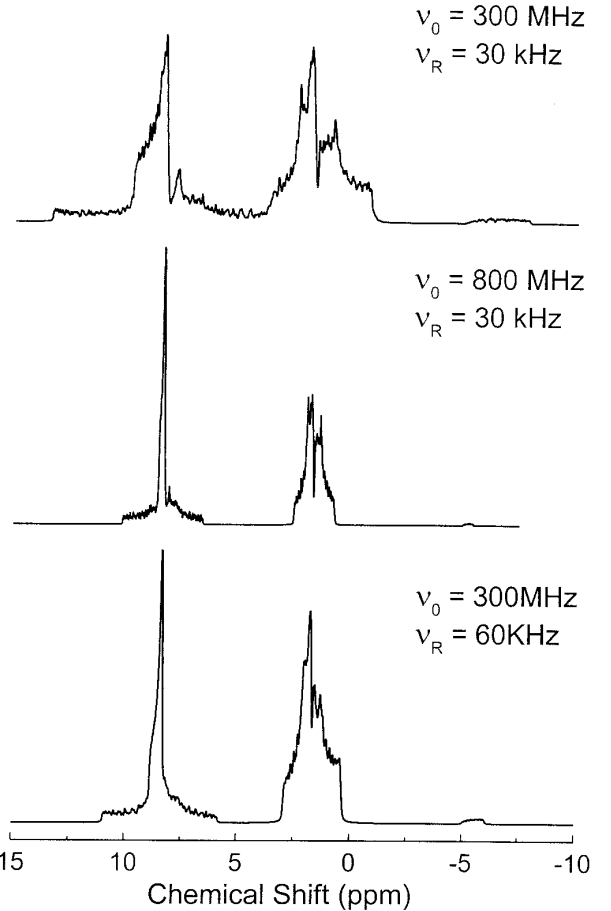
The $M = 1/2$ Floquet matrix can be represented in the manifold of states $\{ |(\alpha\beta\alpha)n\rangle, |(\beta\alpha\alpha)n\rangle, |(\alpha\alpha\beta)n\rangle \}$. Its diagonal elements are equal to $n\omega_R + 1/2\delta_2$, $n\omega_R + 1/2\delta_2$,

and $n\omega_R + \delta_1 - 1/2\delta_2$, and the diagonalization of the z blocks leaves these elements unchanged

$$\begin{aligned}
 \lambda_n^1(1/2) &= n\omega_R + 1/2\delta_2 \\
 \lambda_n^2(1/2) &= n\omega_R + 1/2\delta_2 \\
 \lambda_n^3(1/2) &= n\omega_R + \delta_1 - 1/2\delta_2.
 \end{aligned}
 \quad [A10]$$

The nonzero off-diagonal elements of H_F , which are significant for our discussion, become, to first order in $1/\omega_R$, equal to $((p, q) = (1, 2), (2, 3), (1, 3)$ and $\psi_1 = \alpha\beta\alpha, \psi_2 = \beta\alpha\alpha, \psi_3 = \alpha\alpha\beta$),

$$\begin{aligned}
 &\langle \lambda_n^p(1/2) | H_F | \lambda_n^q(1/2) \rangle \\
 &\cong \sum_k \frac{1}{k\omega_R} \{ \langle \psi_p 0 | H_F | \psi_q k \rangle \langle \psi_q k | H_F | \psi_q 0 \rangle \\
 &\quad + \langle \psi_q 0 | H_F | \psi_p k 0 \rangle^* \langle \psi_p k | H_F | \psi_p 0 \rangle^* \},
 \end{aligned}
 \quad [A11]$$



[A8]

FIG. 8. The simulated centerband of the proton MAS powder spectrum of a three-proton system $\text{H}_2^1\text{-H}^2$, with $r_{1,1,2} = 1.5 \text{ \AA}$, $r_{1,2} = r_{1,2} = 2.7 \text{ \AA}$. Spectra of 1154 crystal orientations were evaluated and added together to form the powder spectra. This number was not enough, even after a broadening of 20 Hz, to eliminate the fluctuations in the spectra. The top spectrum was calculated for a 300-MHz external field and a spinning frequency of 30 kHz. For the middle spectrum the field was increased to 800 MHz and for the bottom spectrum the spinning frequency was increased to 60 kHz. Part of the line narrowing in the middle spectrum is due to the fact that the spectra are presented in a ppm scale.

where we again used the expansions for the diagonalization matrix elements as in Eq. [A4]. The elements in Eq. [A11] connect the diagonal elements in Eq. [A10] and cause a spinning frequency-dependent shift of the Floquet energies. For dipolar terms in the Hamiltonian that are much smaller than the spinning frequency and the chemical shift differences, perturbation theory predicts that the principal eigenvalues of the $M = 1/2$ manifold become about equal to

$$\begin{aligned}\lambda_n^1(1/2) &\cong n\omega_R + 1/2\delta_2 + 1/2\langle\lambda_n^1(1/2)|H_F|\lambda_n^2(1/2)\rangle \\ \lambda_n^2(1/2) &\cong n\omega_R + 1/2\delta_2 - 1/2\langle\lambda_n^1(1/2)|H_F|\lambda_n^2(1/2)\rangle \\ \lambda_n^3(1/2) &\cong n\omega_R + \delta_1 - 1/2\delta_2 \\ &+ 1/\delta_{12} (\langle\lambda_n^3(1/2)|H_F|\lambda_n^1(1/2)\rangle)^2 \\ &+ |\langle\lambda_n^3(1/2)|H_F|\lambda_n^2(1/2)\rangle|^2.\end{aligned}\quad [\text{A12}]$$

Similar results can be derived for the $\{|(M = -1/2)n\rangle\}$ manifold.

This short derivation, and in particular the expressions in Eqs. [A9] and [A12], predicts that part of the shifts of the H_2^1 transitions (1) and (2) are inversely proportional to ω_R and independent of δ_{12} and part of the shifts show a more complicated dependence, of the general form $\{s_1/\omega_R - s_2/(\delta_{12}\omega_R^2)\}$. Thus in a powder MAS spectrum the spectral bandwidth does not follow some simple power dependence on ω_R . Those parts of the spectrum that are independent of δ_{12} will show narrowing only for an increase of the magnetic field when the spectrum is represented in a ppm scale.

To check numerically the spinning frequency dependence of the proton line positions in the three-spin MAS spectrum, the three-proton system $H_2^1-H^2$ was oriented in the rotor frame at some arbitrary orientations and the eight principal eigenvalues were evaluated. In Fig. 7 the dependence of six of these values on $\nu_R = \omega_R/2\pi$ and δ_{12} for a typical single orientation is shown. The two missing values are constant. As can be seen the other values follow the predictions of Eqs. [11] and [12]. The spin parameters of the $H_2^1-H^2$ crystallite were $r_{1,2} = r_{1,2} = 2.7 \text{ \AA}$ and $r_{1,1,2} = 1.5 \text{ \AA}$ and the simulations were performed with $N_f = 21$. In Fig. 8 centerbands of the MAS powder spectra are shown for different fields and spinning frequency. The fluctuations in the spectra are due to the restricted number of 1154 orientations that were taken into account for the powder integration. A line broadening of 20 Hz was applied.

ACKNOWLEDGMENTS

This work was supported by the Israeli Science Foundation. The authors thank Dr. R. Wind and Dr. A. J. Vega for fruitful discussions concerning the proton linewidths in MAS experiments.

REFERENCES

1. A. Mehta, B. Tounge, S. Burns, X. Wu, I. Wu, and K. W. Zilm, in 38th Rocky Mountain Conference on Analytical Chemistry, Denver, 1996.
2. L. M. Ryan, R. E. Taylor, A. J. Paff, and B. C. Gerstein, *J. Chem. Phys.* **72**, 508–515 (1980); G. E. Maciel, C. E. Bronnimann, and B. L. Hawkins, *Adv. Magn. Reson.* **14**, 125–150 (1990).
3. D. E. Demco, S. Hafner, and H. W. Spiess, *J. Magn. Reson. A* **116**, 36–45 (1995).
4. A. Bielecki, A. C. Kolbert, and M. H. Levitt, *Chem. Phys. Lett.* **155**, 341–346 (1989).
5. B.-J. Van Rossum, H. Forster, and H. J. M. de Groot, *J. Magn. Reson.* **124**, 516–519 (1997).
6. H. Geen, J. J. Titmann, J. Gottwald, and H. W. Spiess, *J. Magn. Reson. A* **114**, 264–267 (1995).
7. O. Weintraub and S. Vega, *J. Magn. Reson. A* **105**, 245–267 (1993).
8. T. Nakai and C. A. McDowell, *Mol. Phys.* **77**, 569–584 (1992); T. Nakai and C. A. McDowell, *J. Chem. Phys.* **96**, 3452–3466 (1992).
9. D. Marks and S. Vega, *J. Magn. Reson. A* **118**, 157–172 (1996).
10. M. M. Maricq and J. S. Waugh, *J. Chem. Phys.* **70**, 3300–3316 (1979).
11. M. H. Levitt, D. P. Raleigh, F. Creuzet, and R. G. Griffin, *J. Chem. Phys.* **92**, 6347–6364 (1990).
12. R. Wind, in "Modern NMR Techniques and Their Application in Chemistry" (A.I. Popov and K. Hallenda, Eds.), p. 125; R. Wind, private communication.
13. R. Challoner and C. A. McDowell, *J. Magn. Reson.* **98**, 123–133 (1992).
14. E. Brunner, D. Freude, B. C. Gerstein, and H. Pfeifer, *J. Magn. Reson.* **90**, 90–99 (1990).
15. A. Schmidt and A. Vega, *J. Chem. Phys.* **96**, 2655–2680 (1992).
16. E. Bennet, R. G. Griffin, and S. Vega, in "NMR, Basic Principles and Progress" (P. Diehl, E. Fluck, H. Gunther, R. Kosfeld, and J. Seeling, Eds.), Vol. 33, p. 1, Springer-Verlag, Berlin (1994).
17. H. Conroy, *J. Chem. Phys.* **47**, 5307–5318 (1967).
18. T. O. Levante, M. Baldus, B. H. Meier, and R. R. Ernst, *Mol. Phys.* **86**, 1195–1211 (1995).
19. S. Zhang, *J. Magn. Reson. A* **110**, 73–76 (1994); O. B. Peersen, X. Wu, and S. O. Smith, *J. Magn. Reson. A* **106**, 127–131 (1994); O. B. Peersen, X. Wu, I. Kustanovich, and S. O. Smith, *J. Magn. Reson. A* **104**, 334–339 (1993).
20. S. Zhang, B. H. Meier, and R. R. Ernst, *J. Magn. Reson.* **108**, 30–37 (1994); S. Hediger, B. H. Meier, N. D. Kurur, G. Bodenhausen, and R. R. Ernst, *Chem. Phys. Lett.* **223**, 283–288 (1994); S. Hediger, B. H. Meier, and R. R. Ernst, *Chem. Phys. Lett.* **240**, 449–456 (1995); A. Verhoeven, R. Verel, and B. H. Meier, *Chem. Phys. Lett.* **266**, 465–472 (1997); M. Baldus, D. G. Geurts, S. Hediger, and B. H. Meier, *J. Magn. Reson.* **118**, 140–144 (1996).
21. D. Suter and R. R. Ernst, *Phys. Rev. B* **32**, 5608–5627 (1985).
22. D. E. Demco, J. Tegenfeldt, and J. S. Waugh, *Phys. Rev. B* **11**, 4133–4151 (1975); D. Suter and R. R. Ernst, *Phys. Rev. B* **25**, 6038–6041 (1982); S. R. Hartmann and E. L. Hahn, *Phys. Rev.* **128**, 2042–2053 (1962); F. M. Lurie and C. P. Slichter, *Phys. Rev. A* **133**, 1108–1122 (1964); A. Pines, M. G. Gibby, and J. S. Waugh, *J. Chem. Phys.* **59**, 569–590 (1973); M. Mehring, "Principles of High Resolution NMR in Solids," 2nd ed., Springer-Verlag, Berlin/New York (1983); D. Michel and F. Engelke, in "NMR, Basic Principles and Progress" (P. Diehl, E. Fluck, H. Gunther, R. Kosfeld, and J. Seeling, Eds.), Vol. 32, p. 69, Springer-Verlag, Berlin (1994).